Am J Physiol Regul Integr Comp Physiol 296: R1–R8, 2009.
First published October 29, 2008; doi:10.1152/ajpregu.00078.2008.

CALL FOR PAPERS | *Physiological and Molecular Mechanisms Implicated in the Neural Control of Circulation*

Scavenging superoxide selectively in mouse forebrain is associated with improved cardiac function and survival following myocardial infarction

Timothy E. Lindley,[1]* David W. Infanger,[1,4]* Mark Rishniw,[4] Yi Zhou,[4] Marc F. Doobay,[1] Ram V. Sharma,[1,4,5] and Robin L. Davisson[1,2,3,4,5]

[1]*Department of Anatomy and Cell Biology,* [2]*Free Radical and Radiation Biology Program, Department of Radiation Oncology,* [3]*The Cardiovascular Center, The University of Iowa Roy J. and Lucille A. Carver College of Medicine, Iowa City, Iowa;* [4]*Department of Biomedical Sciences, College of Veterinary Medicine, Cornell University, Ithaca, New York; and* [5]*Department of Cell and Developmental Biology, Weill Cornell Medical College, Cornell University, New York, New York*

Submitted 1 February 2008; accepted in final form 27 October 2008

Lindley TE, Infanger DW, Rishniw M, Zhou Y, Doobay MF, Sharma RV, Davisson RL. Scavenging superoxide selectively in mouse forebrain is associated with improved cardiac function and survival following myocardial infarction. *Am J Physiol Regul Integr Comp Physiol* 296: R1–R8, 2009. First published October 29, 2008; doi:10.1152/ajpregu.00078.2008.—Dysregulation in central nervous system (CNS) signaling that results in chronic sympathetic hyperactivity is now recognized to play a critical role in the pathogenesis of heart failure (HF) following myocardial infarction (MI). We recently demonstrated that adenovirus-mediated gene transfer of cytoplasmic superoxide dismutase (Ad-Cu/ZnSOD) to forebrain circumventricular organs, unique sensory structures that lack a blood-brain barrier and link peripheral blood-borne signals to central nervous system cardiovascular circuits, inhibits both the MI-induced activation of these central signaling pathways and the accompanying sympathoexcitation. Here, we tested the hypothesis that this forebrain-targeted reduction in oxidative stress translates into amelioration of the post-MI decline in myocardial function and increase in mortality. Adult C57BL/6 mice underwent left coronary artery ligation or sham surgery along with forebrain-targeted gene transfer of Ad-Cu/ZnSOD or a control vector. The results demonstrate marked MI-induced increases in superoxide radical formation in one of these forebrain regions, the subfornical organ (SFO). Ad-Cu/ZnSOD targeted to this region abolished the increased superoxide levels and led to significantly improved myocardial function compared with control vector-treated mice. This was accompanied by diminished levels of cardiomyocyte apoptosis in the Ad-Cu/ZnSOD but not the control vector-treated group. These effects of superoxide scavenging with Ad-Cu/ZnSOD in the forebrain paralleled increased post-MI survival rates compared with controls. This suggests that oxidative stress in the SFO plays a critical role in the deterioration of cardiac function following MI and underscores the promise of CNS-targeted antioxidant therapy for the treatment of MI-induced HF.

heart failure; antioxidant gene therapy; survival; sympathetic nervous system

CORONARY ARTERY DISEASE LEADING to myocardial ischemia and infarction (MI) is the primary cause of chronic heart failure (HF) (20). Early after an acute MI, neural and humoral compensatory mechanisms act to maintain adequate perfusion to vital organs (25). Over time, however, a gradual loss of cardiomyocytes due to apoptosis results in myocyte slippage and mural thinning, causing a chronic deterioration in cardiac function that culminates in HF (17, 22). Despite advances in the diagnosis and treatment of heart disease, MI-induced HF continues to be a leading cause of morbidity and mortality in the United States (20).

Abnormalities in central nervous system (CNS) signaling, resulting in excessive sympathetic drive, is strongly implicated in the post-MI decline to HF (7, 13, 35). This neuro-cardiovascular dysfunction increases the risk of cardiac arrhythmias during HF and is positively correlated with mortality (7). Increased plasma norepinephrine levels are a strong predictor of poor prognosis (7), and causal links between chronic sympathoexcitation, cardiomyocyte apoptosis, and heart failure have recently been established (6, 17, 26).

Oxidative stress has received considerable attention recently as an important mechanism in the pathogenesis of HF. Elevated levels of reactive oxygen species (ROS) and decreased amounts of antioxidants have been observed in the plasma and tissues of HF patients (23). Excessive ROS are known to impair cardiac performance, and systemic antioxidants attenuate the development of HF in several different animal models (23). An important concept to emerge recently is that redox mechanisms in the CNS may play a critical role in the pathophysiology of neurocardiovascular diseases (12, 13, 35). Zanzinger and Czachurski (29) first demonstrated that microinjection of the ROS scavenger superoxide dismutase (SOD) into the brain stem decreased the exaggerated sympathetic tone in pigs receiving chronic nitrate therapy. Our studies have shown that excessive superoxide production in the CNS mediates neurogenic ANG-II-dependent hypertension in mice (33), and others have demonstrated that this is due to ROS-mediated increases in sympathoexcitation (15, 35). Furthermore, we have shown that ROS scavenging in forebrain circumventricular organs (CVOs), particularly the subfornical organ (SFO),

* These authors contributed equally to this article.

Address for reprint requests and other correspondence: R. L. Davisson, Biomedical Sciences, College of Veterinary Medicine, and Cell & Developmental Biology, Weill Cornell Medical College, T9-014 Veterinary Research Tower, Cornell Univ., Ithaca, NY 14853-6401 (e-mail: rld44@cornell.edu).

The costs of publication of this article were defrayed in part by the payment of page charges. The article must therefore be hereby marked "*advertisement*" in accordance with 18 U.S.C. Section 1734 solely to indicate this fact.

diminishes the post-MI-induced sympathoexcitation in HF (14). Zucker and colleagues (9) have showed that NADPH oxidase activity in the rostral ventrolateral medulla (RVLM), a brain stem nucleus that links the forebrain CVOs with increased sympathetic outflow, plays an important role in the sympathoexcitation observed in a rabbit model of chronic heart failure.

Given the importance of sympathetic hyperactivity in the development of HF, along with recent findings that central oxidative stress is involved in driving central autonomic dysfunction, here we tested the hypothesis that selective forebrain-targeted scavenging of ROS ameliorates the post-MI decline in myocardial function. We used a mouse model of MI and adenoviral vectors to cause long-term modulation of the redox state, and our results demonstrated that scavenging ROS in the SFO led to improved myocardial function. This was accompanied by diminished levels of cardiomyocyte apoptosis and increased post-MI survival. These findings suggest that antioxidant strategies directed at CNS cardiovascular control regions may provide a novel therapeutic approach for the treatment of MI-induced HF.

MATERIALS AND METHODS

Animals. Adult male C57BL/6 mice (8 wk) were used for all experiments. Animals were fed standard chow (Harlan Laboratories) and water ad libitum. All procedures were approved by the Animal Care and Use Committee at The University of Iowa and Cornell University. Care of the mice met or exceeded the standards set forth by the National Institutes of Health *Guide for the Care and Use of Laboratory Animals*, U.S. Department of Agriculture regulations, and the American Veterinary Medical Association Panel on Euthanasia.

Myocardial infarction and CNS viral gene transfer. MI was induced by ligation of the left anterior descending (LAD) coronary artery as described in detail previously (14). Briefly, mice were anesthetized, intubated, and ventilated. The heart was exposed via the third intercostal space, and the LAD was ligated using 8–0 Ethilon suture. The thoracic wall was closed, and the mice were extubated. Sham-operated animals underwent the same procedure, except the LAD was not ligated. During the same surgical session, mice then underwent intracerebroventricular injections of titer-matched stocks of adenoviral vectors (1×10^9 pfu/ml, 500 nl), encoding either human cytoplasmic Cu/Zn superoxide dismutase (Ad-Cu/ZnSOD) or control β-galactosidase (Ad-LacZ). We have previously demonstrated that intracerebroventricular delivery results in robust gene transfer to SFO 100% of the time, with very occasional transduction of another forebrain CVO, the organum vasculosum of the lamina terminalis (OVLT) (<5% of the time) (21). At the conclusion of the experiments, SOD expression was localized by immunohistochemistry in brain sections using a sheep anti-human Cu/ZnSOD antibody (1:200; The Binding Site, Birmingham, UK) as described by Zimmerman et al. (32). Images were collected digitally using a Nikon Labphot-2 Microscope equipped with epifluorescence and a Pixera 600 imaging system.

Analysis of brain superoxide levels. A subset of mice were killed 2 wk after surgery, and the brains were removed and immediately frozen on dry ice for measurement of superoxide levels, as described previously (34). Briefly, brains were cryosectioned (30 μm) onto glass slides, rinsed in PBS for 5 min, and incubated in 1 μM of dihydroethidium (DHE; in PBS) for 5 min in the dark. Slides were then rinsed in PBS for 2 min and imaged using confocal microscopy (Zeiss LSM 510) using an excitation wavelength of 543 nm and a rhodamine emission filter. DHE-treated tissues for all groups were processed and analyzed in parallel with identical detector and laser settings. Fluorescence intensity in the SFO was analyzed using Image J software as described (34). All data are expressed relative to sham animals.

Hemodynamic measurements. Hemodynamic measurements were performed as described (16, 18) at 2 and 4 wk following MI or sham surgery. Mice were anesthetized with pentobarbital sodium (25 mg/kg ip), and a 1.4F Millar catheter (Millar Instruments, Houston, TX) was inserted into the left ventricle (LV) via the right common carotid artery under the guidance of the pressure signal as described (16). LV pressures were recorded for 10 min, data were digitized (Power Lab, Chart Version 4.01), and $dP/dt+$ and $dP/dt-$ were calculated as an index of myocardial contractility as described by Martinka et al. (18). The time series for LV pressure were interpolated using the cubic spline method (4) to a new sampling rate of 2,000 Hz to obtain more accurate estimates of $dP/dt+$ and $dP/dt-$.

Determination of cardiac mass and infarct size. At the conclusion of the hemodynamic studies, mice were weighed and then killed. Hearts were removed, blotted of excess blood, and weighed. Cardiac mass is expressed as a ratio of heart weight to body weight (mg/g). Hearts were then cryosectioned (short axis, 20 μm), mid-LV sections were mounted onto glass slides, and samples were counterstained with hematoxylin and eosin. Digital images of the sections were acquired, and Scion Image (Scion) was used to determine the infarct size, as described previously (14).

Echocardiography. Transthoracic echocardiography was performed in a separate subset of mice using a Vevo 770 high-resolution imaging system (VisualSonics, Toronto, Canada) under isoflurane (1%) anesthesia. Excess hair was removed from the thoracic region with chemical treatment (Nair, Church & Dwight, Princeton, NJ) to minimize signal attenuation. Images were acquired using a single-element mechanical transducer with broadband frequency of 45 MHz coupled to the chest using warmed Aquasonic 100 transmission gel (Parker Labs, Fairfield, NJ). Parasternal long and short axis (mid-papillary level) retrospective B-mode cineloops were acquired for analysis (1). Fractional shortening (FS) was calculated as [(LV end diastolic dimension − LV end systolic dimension)/LV end diastolic dimension·100]. Because of LV asymmetry, which occurs after infarction, LV end-diastolic volume (LVEDV) and LV end systolic volume (LVESV) were measured from the parasternal long-axis view and calculated using Simpson's formula (3). Ejection fraction (EF) was calculated as [(LVEDV − LVESV)/(LVEDV)·100]. To calculate infarct size, length of infracted myocardium was measured from the parasternal short axis view and expressed as a percentage of the left ventricle circumference.

Quantification of apoptotic nuclei using terminal deoxynucleotidyl transferase dUTP-mediated nick-end labeling assay. Alternating mid-LV cryosections were mounted on poly-L-lysine-coated slides (Sigma, St. Louis, MO), and terminal deoxynucleotidyl transferase dUTP-mediated nick-end labeling (TUNEL) assays were performed using ApopTag Plus peroxidase in situ apoptosis detection kit (Serologicals, Norcross, GA), according to the manufacturer's instructions. As a positive control, sections were treated with DNase I to enzymatically induce the formation of DNA strand breaks. Negative control samples underwent the same protocol except biotin-16-dUTP or terminal deoxynucleotidyl transferase was not included in assays performed on DNase I-treated sections. The apoptotic index was determined by dividing the number of nuclei labeled by biotinylated dUTP by the total number of nuclei per unit area of tissue (outside of the infarct and peri-infarct zones) in three randomly selected fields per LV section (three sections per sample) analyzed by a blinded observer. All data are expressed relative to sham animals.

Quantification of apoptosis using DNA laddering. Hearts were removed from a separate cohort of mice from each of the treatment groups (2 wk time point) and placed on ice. Peri-infarct and noninfarct LV tissue was collected using a dissection microscope and immediately frozen on dry ice. Genomic DNA was isolated and quantified (Nanodrop 1000). Apoptotic fragments were enriched using dephosphorylated adaptor molecules ligated to 0.3 μg DNA followed by hot

start PCR, according to manufacturer instructions (APO-DNA1, Maxim Biotech, San Francisco, CA). PCR products were run on a 1.5% agarose gel and visualized under UV light. 200-, 400-, 600-, and 800-bp band densities were quantitated using Image J software (National Institutes of Health, Bethesda, MD).

Statistical analyses. All data are expressed as means ± SE and were analyzed by ANOVA (after Bartlett's test of homogeneity of variance) followed by the Newman-Keuls correction for multiple comparisons using Prism (GraphPad Software, San Diego, CA). We compared the proportion of MI mice that survived between treatment groups using Fisher's Exact Test.

RESULTS

MI increases superoxide radical formation in the SFO. We first performed DHE fluorescence microscopy to directly examine superoxide levels in brains of MI and sham mice. As seen in the representative photomicrograph in Fig. 1*A* and the summary data in Fig. 1*B*, MI caused a nearly seven-fold increase in superoxide-mediated fluorescence in SFO of control vector-treated mice compared with sham animals at 2 wk. Comparable changes in ROS were not observed in any other brain region. Ad-Cu/ZnSOD abolished the ROS increase in SFO (Fig. 1, *A* and *B*), providing corroborating evidence that the free radical generated in this brain region is cytoplasmic superoxide. We further confirmed effective Ad-mediated gene transfer of Cu/ZnSOD to the SFO by performing immunohistochemistry following our experiments. As shown in Fig. 1*C*, Cu/ZnSOD is expressed at a high level throughout the SFO of Ad-Cu/ZnSOD-treated mice compared with extremely low levels of background staining in Ad-LacZ-treated mice. Transduction of other forebrain structures was not observed.

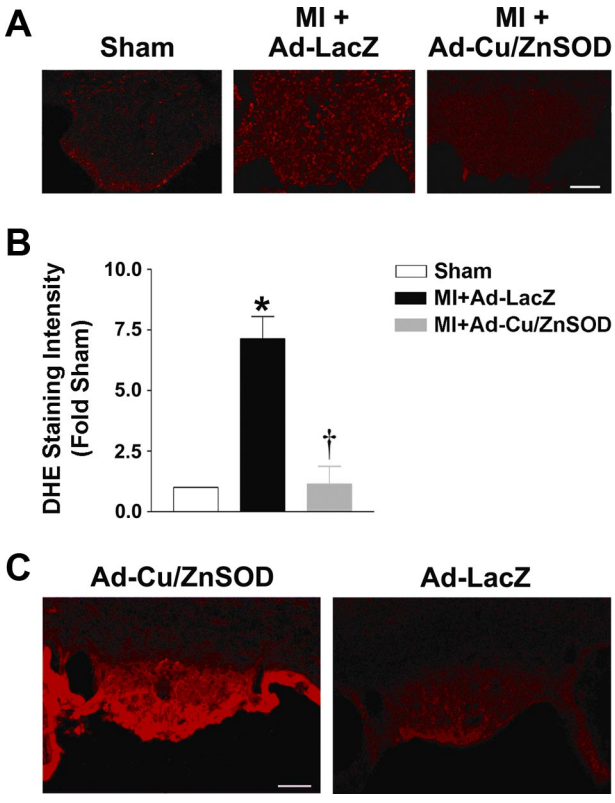

Fig. 1. Myocardial infarction (MI) increases superoxide formation in the subfornical organ (SFO) of mouse brain. *A*: representative photomicrographs of dihydroethidium (DHE) staining in the SFO of sham mice and MI mice that underwent intracerebroventricular microinjection of Ad-Cu/ZnSOD or Ad-LacZ. *B*: summary of DHE fluorescence intensity in the SFO, demonstrating a ~7-fold increase in superoxide-mediated fluorescence in this brain region of MI mice (MI+Ad-LacZ, $n = 5$) compared with shams ($n = 3$). Ad-Cu/ZnSOD ($n = 5$) abolished this increase. Three coronal sections (30 μM) through the SFO from each animal were analyzed. *$P < 0.05$ vs. sham; †$P < 0.05$ vs. MI+Ad-LacZ. *C*: typical immunostaining of SFO showing robust human Cu/ZnSOD expression in mice that underwent intracerebroventricular injections of Ad-Cu/ZnSOD (*left*) 2 wk earlier, but not in Ad-LacZ-injected mice (*right*). Scale bar = 50 μm.

Forebrain-targeted superoxide scavenging is associated with improved myocardial function following MI. We next examined whether forebrain targeting of AdCu/ZnSOD translates into improved cardiac performance. Coronary ligation resulted in hemodynamic changes indicative of LV dysfunction (Fig. 2*A*). Because there were no differences within groups at the two time points, the data were combined. Compared with sham animals, MI mice exhibited a marked decrease in left ventricular peak systolic pressure (LVSP), as well as impairment in LV contraction and relaxation (±d*P*/d*t*). Gene transfer of the control vector Ad-LacZ had no effect on these responses (Fig. 2*B*). In contrast, mice that had undergone forebrain-targeted gene transfer of Ad-Cu/ZnSOD at the time of coronary ligation had significantly improved cardiac performance, such that the LVSP and ± d*P*/d*t* were not significantly different from sham animals (Fig. 2*B*). Interestingly, we did not observe any significant increases in LV end-diastolic pressure (LVEDP) in MI mice compared with sham-operated controls, nor was this parameter affected by CNS gene transfer of Ad-Cu/ZnSOD (Fig. 2*B*). Similarly, but less surprisingly, there were no significant differences in heart rate between groups (sham, 430 ± 24; MI, 418 ± 21; MI + AdLacZ 421 ± 21; MI + Ad-Cu/ZnSOD 468 ± 20 bpm, $n = 9$–11 per group, $P > 0.05$).

High-resolution echocardiography was also performed 48 h after surgery to confirm successful arterial ligation and to quantitate "baseline" infarct sizes, indicated by akinetic wall motion along the anterolateral border of the LV (images not shown). In addition, a similar extent of infarction was observed across the various treatment groups (percent of wall infarcted in short axis: MI, 26.6 ± 1.6%, $n = 12$; MI + Ad-LacZ, 28.9 ± 2.6%, $n = 7$; MI+Ad-Cu/ZnSOD, 28.7 ± 0.9%, $n = 11$; $P > 0.05$). A summary of LV function data combined from measurements taken between 2 and 4 wk following sham or MI procedure is shown in Fig. 3. It should be noted that as with the hemodynamic study above, the data were combined across the 2- to 4-wk period since there were no significant differences within the groups at the different time points. LAD ligation caused marked reductions in FS (Fig. 3*A*) and EF (Fig. 3*B*), indicating severe impairment of LV contractility. Importantly, Ad-Cu/ZnSOD significantly improved both of these indices compared with the control vector, suggesting that increased redox signaling in SFO contributes to declining cardiac performance during HF. MI also caused significant increases in end-systolic and diastolic volumes, (Fig. 3, *C* and *D*), further demonstrating impaired LV contraction, as well as chamber enlargement. While LVESV was significantly reduced in MI mice treated with Ad-Cu/ZnSOD (Fig. 3*C*), there was no significant effect of treatment on LVEDV (Fig. 3*D*). Finally, similar to results from the catheterization studies, HR was not significantly different [sham + Ad-LacZ, 431 ± 9 beats per minute (bpm); MI+Ad-LacZ, 426 ± 16 bpm; MI+Ad-Cu/

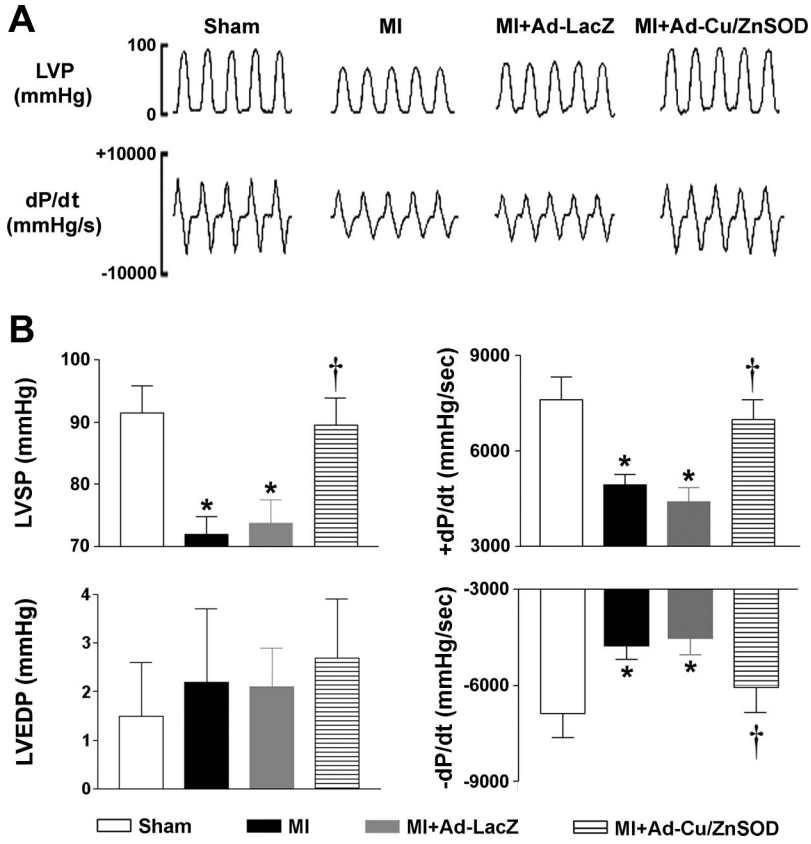

Fig. 2. Increased scavenging of superoxide in the forebrain improves myocardial function following MI. *A*: representative high-fidelity recordings of left ventricular pressure (LVP) obtained with a 1.4F Millar catheter in sham, MI, and MI mice that underwent intracerebroventricular injection of Ad-Cu/ZnSOD or Ad-LacZ. *B*: summary data showing that MI resulted in significant reductions in LV peak systolic pressure (LVSP) and impairment in LV contraction/relaxation (+/−dP/d*t*) (MI, $n = 9$ or MI+AdLacZ, $n = 10$ vs. shams, $n = 9$). Myocardial function was significantly improved in MI mice that underwent gene transfer of Ad-Cu/ZnSOD ($n = 11$). There were no differences in LVEDP. *$P < 0.05$ vs. sham. †$P < 0.05$ vs. MI or MI+Ad-LacZ.

ZnSOD 447 ± 15 bpm, $n = 11$–14 per group, $P > 0.05$], suggesting that differences in LV performance between groups were not due to the effects of anesthesia.

Despite the improvement in function in Ad-Cu/ZnSOD-treated mice, MI-induced increases in cardiac mass (sham, 4.8 ± 0.2; MI, 6.8 ± 0.5, $n = 9$–11 per group, $P < 0.05$) were not differentially affected in this group compared with Ad-LacZ-treated animals (MI+Ad-LacZ, 7.6 ± 0.4; MI+Ad-Cu/ZnSOD, 6.8 ± 0.3, $n = 9$–11 per group, $P > 0.05$). Infarct sizes were also similar in all MI groups both by hematoxylin-and-eosin staining of cardiac sections (MI, 53.9 ± 3.6%; MI+Ad-LacZ, 53.8 ± 2.8%; MI+Ad-Cu/ZnSOD, 55.4 ± 2.5%, $n = 9$–11 per group, $P > 0.05$) and by echocardiography at 2 wk (MI, 43.9 ± 1.3%, $n = 12$; MI+Ad-LacZ, 43.9 ± 3.1%, $n = 9$; MI+Ad-Cu/ZnSOD, 42.6 ± 1.3%, $n = 11$, $P > 0.05$).

Overexpression of Cu/ZnSOD in the forebrain decreases cardiomyocyte apoptosis following MI. We hypothesized that decreased apoptosis in the surviving myocardium may account for the improved myocardial function in Ad-Cu/ZnSOD-treated MI mice, and we, therefore, performed TUNEL assays to identify apoptotic nuclei. As shown in the representative photomicrographs and summary data in Fig. 4, MI treatment markedly increased the cardiomyocyte apoptosis compared with sham, which was significantly reduced in MI-treated mice receiving central gene transfer of Cu/ZnSOD.

We also performed DNA laddering experiments to confirm the results of the TUNEL assay. As shown in Fig. 4, *C* and *D*, MI caused ~3.5-fold increases in DNA laddering, which was significantly reduced by Ad-Cu/ZnSOD. These effects were largely restricted to the peri-infarct border of the left ventricle, as noninfarcted myocardium from all treatment groups exhibited virtually no DNA laddering (data not shown). Together, these results support a role for central redox signaling in the increased myocardial apoptosis seen after MI.

Viral gene transfer of Cu/ZnSOD to the forebrain decreases mortality following MI. There were dramatic differences in long-term post-MI survival between experimental groups. Of all of the mice that underwent the MI procedure, 91.3% (63 of 69) survived the initial postsurgery period. However, by 7 days postsurgery, ~30% (6 of 20) of MI-only treated mice had died (Fig. 5). Similar mortality rates were observed in the MI mice that received control vector (6 of 21, 30%) (Fig. 5). Interestingly, there was no additional mortality observed between 2 and 4 wk in either MI treatment group (data not shown). Upon necroscopic inspection, all of the animals that died showed a large accumulation of blood in the thoracic cavity, suggesting left ventricular rupture. In contrast, only 5% (1 of 22) of the Ad-Cu/ZnSOD-treated MI mice died during this time period (Fig. 5), with 21 of 22 of these mice surviving to the conclusion of the experiments, suggesting that increased superoxide scavenging in the brain protected mice from the deleterious effects of MI.

DISCUSSION

Developing heart failure is associated with unchecked neurohumoral excitation that progressively fuels cardiovascular deterioration (13, 25). Mounting evidence implicates the CNS as a primary culprit in driving this neural dysfunction (7, 13, 35). We have shown that superoxide radicals in the brain play a key role in the excessive sympatho excitation that occurs

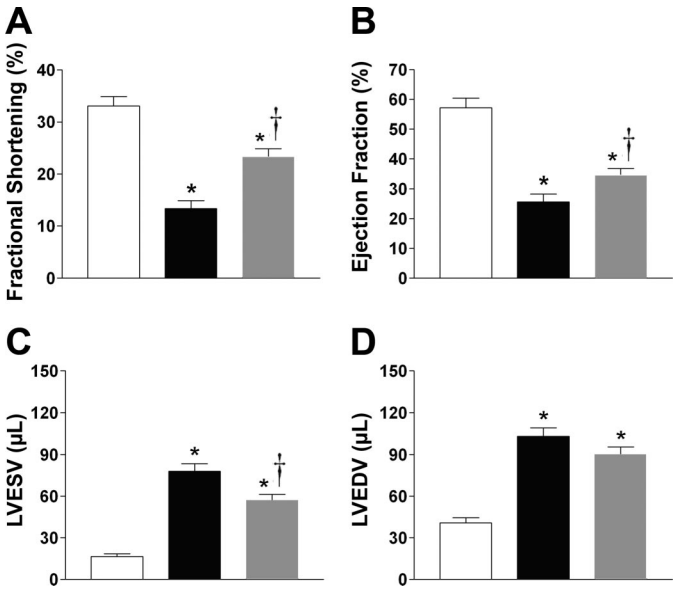

Fig. 3. Forebrain-targeted overexpression of Cu/ZnSOD improves LV function following MI. Summary of echocardiography data collected 2–4 wk following MI or sham and SFO gene transfer. MI ($n = 27$) caused significant decreases in fractional shortening (*A*) and ejection fraction (*B*) compared with shams ($n = 17$), and overexpression of Cu/ZnSOD in the forebrain ($n = 28$) caused significant improvement in these two endpoints. The MI-induced increases in end-systolic volume (LVESV) were significantly improved by Cu/ZnSOD (*C*), whereas the LV dilation at end-diastole (LVEDV) was not (*D*). *$P < 0.05$ vs. sham+Ad-LacZ; †$P < 0.05$ vs. MI+Ad-LacZ.

following an MI in mice (14), and we provide here evidence that scavenging increased superoxide formation in the SFO—a pivotal brain region linking peripheral blood-borne signals with CNS cardiovascular circuits—is associated with marked improvement in cardiac performance following MI. Furthermore, we demonstrate that forebrain oxidant scavenging is associated with a decrease in cardiomyocyte apoptosis in the surviving myocardium and increased post-MI survival rates.

Emerging evidence suggests that certain CNS circuits serve as relay centers to integrate input from different organ systems in the periphery and regulate neurohumoral output that plays a crucial role in cardiac dysfunction and remodeling following MI (7, 13, 35). Our results further underscore this notion. Upon binding circulating factors, neurons in the SFO send extensive projections to the hypothalamic paraventricular nucleus (PVN), which plays an integral role in the regulation of vasopressin release and sympathetic tone, both directly and via projections to the RVLM (8, 13). Chronic overactivation of the SFO-PVN axis by ANG-II, aldosterone, interleukins, and tumor necrosis factor-α has been widely implicated in causing the MI-induced sympatho-excitation (7, 10, 28, 30, 31). For example, chronically blocking ANG-II signaling selectively in the brain reduces sympathetic activity, improves cardiac baroreflex function, decreases cardiac hypertrophy, and attenuates the subsequent development of HF following MI (12, 13, 31). Furthermore, central mineralocorticoid blockade reduces sympathetic drive in HF rats (7, 30), and injection of TNF-α into the carotid artery increases sympathetic output (7). Together, these findings suggest that multiple signaling pathways may converge to increase oxidative stress in the SFO following MI, which may, in turn, powerfully influence sympathetic activity and the subsequent deterioration of cardiac function. Our results suggest that interruption of this cascade through targeted scavenging of ROS leads to improved cardiac performance. Further studies will be required to tease out the specific molecular substrates affected by central ROS scavenging and improved cardiac function after MI.

Because we observed a marked improvement in cardiac performance in Ad-Cu/ZnSOD-treated MI mice without observing a significant difference in infarct size or cardiac mass in these animals, we hypothesized that central antioxidant therapy may improve cardiac function by somehow preserving the integrity of the surviving myocardium. In support of this hypothesis, we observed a significant decrease in TUNEL-positive nuclei and DNA laddering in the LV of MI mice that had undergone gene transfer of Ad-Cu/ZnSOD compared with control vector-treated MI mice. Previous studies strongly suggest that apoptosis in the LV plays a critical role in the deterioration in cardiac function following MI, and apoptotic index is positively correlated with the degree of myocardial dysfunction in humans (reviewed in Refs. 17 and 23). Recent studies have also suggested that therapies aimed at diminishing or replacing apoptotic cells in the surviving myocardium improves post-MI cardiac performance (17), even without significantly altering the infarct size. It is well established that increased sympathetic drive induces myocyte apoptosis, and treatment with beta-receptor antagonists decreases apoptosis in the LV in animal models of HF (6, 25, 26). We have previously demonstrated that scavenging superoxide in the brain decreases sympathetic tone following MI in mice (14). Similarly, Gao et al. (9) have demonstrated that intracerebroventricular administration of the antioxidant Tempol or the NADPH oxidase inhibitor apocynin significantly attenuated resting renal sympathetic nerve activity in rabbits with HF (9). Together, these findings suggest central ROS scavenging may be linked to improved cardiac performance through decreasing norepinephrine-mediated cardiomyocyte apoptosis in the post-MI heart.

One interesting question is what advantages targeting SOD to the brain provides over systemic treatment with beta-receptor antagonists. Beta-blockade improves cardiac function and improves survival after MI in animal models (24), and is a mainstay of therapy for MI patients. However, optimal treatment is often limited by poor tolerance in humans due to the associated decrease in HR (5). In contrast, although we previously demonstrated that brain gene transfer of Cu/ZnSOD caused a decrease in markers of global sympathetic tone (14), resting heart rate was not affected. Thus, central ROS scavenging may allow for appropriate blockade of sympathetic tone to the LV without unwanted bradycardia due to direct blockade of beta-receptors in the heart.

Our findings that inhibition of sympathetic output by selectively scavenging central ROS paralleled improvements in cardiac performance and survival is intriguing compared with recent clinical trials in which chronic HF patients treated with the central sympathetic inhibitor moxonidine exhibited elevated mortality compared with HF patients dosed with placebo (2, 19). It is possible that reducing sympathetic output by inhibiting specific redox circuits is beneficial to cardiac function following MI; however, complete and/or nonspecific ablation of central regulatory pathways may preclude autonomic functions that are beneficial to the failing heart. Finally, in addition to regulating sympathetic tone, targeting forebrain cardiovascular control regions may have further therapeutic

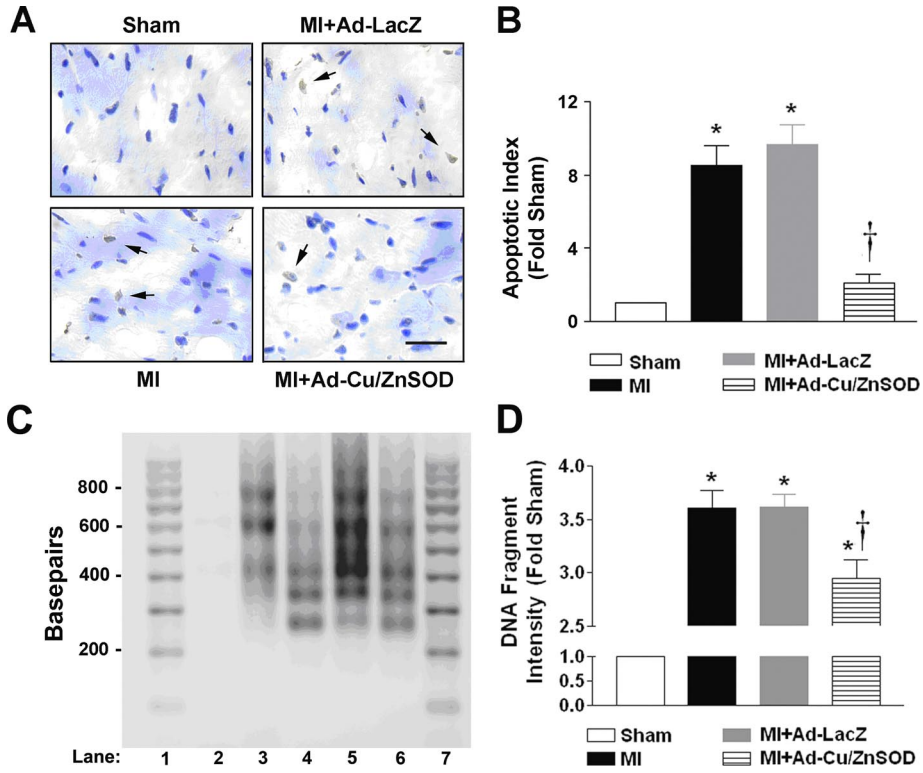

Fig. 4. Central antioxidant therapy is associated with decreased apoptosis in the heart following MI. *A*: representative photomicrographs of terminal deoxynucleotidyl transferase dUTP-mediated nick-end labeling (TUNEL) staining performed on tissue sections from the surviving myocardium of sham, MI, and MI mice treated intracerebroventricularly with Ad-LacZ or Ad-Cu/ZnSOD. *B*: summary data demonstrating that MI ($n = 4$) caused a nearly eight-fold increase in the apoptotic index in myocardial sections compared with shams ($n = 6$). Forebrain-targeted gene transfer of Ad-Cu/ZnSOD ($n = 9$) reduced the number of apoptotic nuclei to near sham levels, whereas Ad-LacZ ($n = 10$) had no effect. *$P < 0.05$ vs. sham. †$P < 0.05$ vs. MI or MI+Ad-LacZ. Scale bar = 25 μm. *C*: apoptotic DNA fragmentation was examined by ligation-mediated PCR and visualized by agarose gel electrophoresis. Shown are fragments isolated from peri-infarct myocardium 2 wk after sham (*lane 2*), MI (*lane 3*), MI + Ad-Cu/ZnSOD (*lane 4*), or MI + Ad-LacZ (*lane 5*). Positive-control DNA provided by the manufacturer is shown in *lane 6*; *lanes 1* and *7* contain molecular-weight ladder. *D*: summary graph of densitometry analysis performed on 200-, 400-, 600-, and 800-base-pair fragments shows an increase in MI-induced ($n = 4$) apoptosis compared with sham ($n = 4$), which was significantly reduced with targeting of Ad-Cu/ZnSOD to the forebrain ($n = 5$). *$P < 0.05$ vs. sham; †$P < 0.05$ vs. MI or MI+Ad-LacZ.

effects. The SFO-PVN-RVLM axis is well known to play a key role in regulating other ROS-sensitive signaling molecules involved in the pathogenesis of HF, including vasopressin, cytokines, and the renin-angiotensin system (7, 10, 13, 28, 30). Therefore, modulation of central ROS signaling may have an important effect on these targets, and this is the focus of ongoing investigations.

Another striking observation in this study is that gene transfer of Cu/ZnSOD to the forebrain improved survival following MI, apparently by decreasing the risk of LV rupture. Although the mechanisms through which central ROS scavenging would protect against MI-induced LV rupture are not understood, the potential interaction between increased sympathetic nerve activity, β-adrenergic signaling and activation of matrix metalloproteinases (MMPs) in the heart is one intriguing possibility (6, 17, 22, 23). For example, it has been demonstrated that there is increased survival after MI in transgenic mice overexpressing an inhibitor of β-adrenergic receptor kinase (24). Moreover, we have observed a rapid increase in MMPs (peak at 3 days) that precedes LV rupture and death in MI mice, and treatment of mice with the SOD-mimetic Tempol at the time of surgery markedly decreases MMP induction, urinary norepinephrine levels, and MI-induced mortality (T. E. Lindley, M. F. Doobay, R. C. Bhalla, R. V. Sharma, R. L. Davisson, unpublished data). Thus, it is possible that Ad-Cu/ZnSOD-mediated decreases in post-MI sympathetic drive may improve survival by decreasing β-adrenergic signaling and MMP induction in the heart.

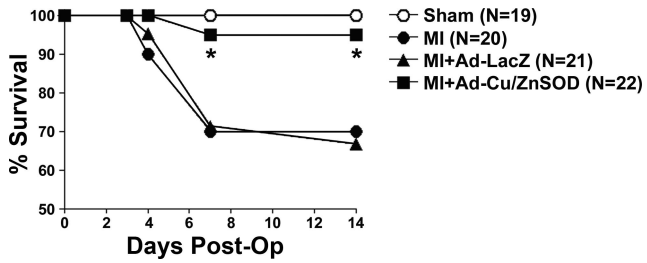

Fig. 5. Ad-mediated gene transfer of Cu/ZnSOD to the forebrain reduces mortality following MI. Summary of percentage of animals surviving the first 2 wk after sham or MI surgery. By *days 4–7* post-MI, ~30% of MI mice had died. Intracerebroventricular injection of Ad-Cu/ZnSOD increased survival in MI mice to nearly the same level as shams, whereas Ad-LacZ had no effect on mortality. There was no mortality among the sham animals. *$P < 0.05$ vs. MI alone or MI+Ad-LacZ; (n given in figure).

Although we made every attempt to include the appropriate controls for all experiments, there are particular variables that we could not control, which therefore limit the conclusions that can be drawn. Hemodynamic and echocardiography measurements made under anesthesia can influence cardiac function, and although we observed no significant differences in heart rates between groups during measurements, the values were nonetheless diminished compared with conscious animals, and this should be taken into account. In addition, there certainly are species-related limitations of our study in mice that need to be considered. For example, our observation of post-MI LV rupture is not reflective of the usual pattern of HF development in humans. Although a typical effect of LAD ligation in mice (11, 27), it should be noted that the beneficial effect of SOD on this particular end point likely does not apply in humans. Similarly, although we have previously shown marked decreases in sympathetic activity (14), and now significant beneficial effects on myocardial function with SOD gene targeting to the forebrain, it should be noted that we cannot definitively conclude that SOD produces these myocardial improvements by only reducing sympathetic tone. As suggested above, it is certainly possible that other ROS-sensitive mechanisms are

operating in parallel and that interruption of these pathways by SOD could contribute to the improvement in cardiac performance. Similarly, while we have shown that intracerebroventricular injection confers robust transgene expression in the SFO 100% of the time but can cause transduction of the OVLT occasionally (<5% of the time), it is conceivable that ROS scavenging in this other region could influence the improved cardiac performance and decreased apoptosis that we observed. However, because we did not observe increased ROS formation in the OVLT, we do not believe that this is likely.

Given the significant LV dysfunction, we observed in our MI-treated mice, we were surprised to see no significant increases in LVEDP relative to sham controls at 2- and 4-wk (Fig. 2*B*). This could be a function of subsequent eccentric hypertrophy of the preserved myocardium over the 2–4 wk post-infarction period, allowing LVEDP to return to near-normal levels at substantially increased LVEDVs. The magnitude of increase in LVEDV (almost threefold) indicates that this was more than just a result of necrotic myocardium and stretch but that compensatory eccentric myocardial hypertrophy was involved. Alternatively, this may have been a technical limitation of our intracardiac instrumentation, whereby a difference between groups of <5 mmHg may exceed the sensitivity threshold. In support of this, our greatest degree of variability between mice of the same treatment group was observed in our LVEDP measurements (Fig. 2*B*).

While intracerebroventricular delivery of Ad-Cu/ZnSOD improved ±dP/d*t*max in MI-treated mice to sham-treated levels, these mice still exhibited significantly reduced EF and elevated LVEDV. However, these can be mutually exclusive—a large EDV does not necessitate a decrease in dP/d*t*max (or other measures of systolic function). Therefore, the rate of cardiomyocyte contraction (measured by dP/d*t*max) can be similar between groups, although the ventricular volumes at which these myocytes start to contract are different. LV contraction from a greater starting volume will result in a decreased EF for any specific stroke volume (which is the ultimate determinant of cardiac output). This explains the minimal change in EF despite an improvement in dP/d*t*max. Similarly, for the LVEDV to decrease, one would need to invoke cardiomyocyte atrophy to a preinfarction state—an unlikely explanation in the face of an infarction involving 45% of the LV wall. The compensatory eccentric hypertrophy may allow reduction of LVEDP to subcritical levels, with a consequent reduction in end-diastolic wall stress. Indeed, our data demonstrate the independence of these two different measures of cardiac function. Finally, the volumes involved in our model may be too small to allow small but significant differences to be detected using echocardiographic estimates of cardiac volume (Simpson's method).

Perspectives and Significance

In conclusion, our results suggest that oxidative stress in the SFO play a prominent role in the neural dysfunction that accompanies HF. The current study provides evidence for the first time that interfering with redox pathways selectively in the forebrain is associated with improved myocardial function, amelioration of cardiac apoptosis, and increased survival following MI. These findings underscore the critical role central redox signaling plays in the deterioration of cardiac function following MI and suggest that antioxidant therapy directed to certain regions of the CNS may provide a novel strategy for the treatment of HF.

ACKNOWLEDGMENTS

The authors would like to thank Dr. Harald Stauss (University of Iowa) for his expert help in analysis of hemodynamic data, Dr. Matthew Zimmerman (University of Nebraska Medical Center) for help with the dihydroethidium studies, and Jack Stupinski for assistance with data analyses. We would also like to thank Paul Reimann and Dennis Dunnwald for expert help with the images.

GRANTS

The work described herein was funded by grants to R. L. Davisson from the National Institutes of Health (NIH) (Grants HL-14388, HL-55006, and HL-63887) and the American Heart Association (AHA) (0540114N). T. E. Lindley was supported by an NIH Institutional (NRSA) (HL07638). D. W. Infanger was supported by an NIH Institutional National Research Service Award (HL07638) and an AHA predoctoral fellowship (0815714D).

REFERENCES

1. **Cherin E, Williams R, Needles A, Liu G, White C, Brown AS, Zhou YQ, Foster FS.** Ultrahigh frame rate retrospective ultrasound microimaging and blood flow visualization in mice in vivo. *Ultrasound Med Biol* 32: 683–691, 2006.
2. **Cohn JN, Pfeffer MA, Rouleau J, Sharpe N, Swedberg K, Straub M, Wiltse C, Wright TJ, Investigators MOXCON.** Adverse mortality effect of central sympathetic inhibition with sustained-release moxonidine in patients with heart failure (MOXCON). *Eur J Heart Fail* 5: 659–667, 2003.
3. **Collins KA, Korcarz CE, Lang RM.** Use of echocardiography for the phenotypic assessment of genetically altered mice. *Physiol Genomics* 13: 227–239, 2003.
4. **Daskalov I, Christov I.** Improvement of resolution in measurement of electrocardiogram RR intervals by interpolation. *Med Eng Phys* 19: 375–379, 1997.
5. **DiBianco R.** Update on therapy for heart failure. *Am J Med* 115: 480–488, 2003.
6. **Ellison GM, Torella D, Karakikes I, Purushothaman S, Curcio A, Gasparri C, Indolfi C, Cable NT, Goldspink DF, Nadal-Ginard B.** Acute beta-adrenergic overload produces myocyte damage through calcium leakage from the ryanodine receptor 2 but spares cardiac stem cells. *J Biol Chem* 282: 11397–11409, 2007.
7. **Felder RB, Francis J, Zhang ZH, Wei SG, Weiss RM, Johnson AK.** Heart failure and the brain: new perspectives. *Am J Physiol Regul Integr Comp Physiol* 284: R259–R276, 2003.
8. **Ferguson AV, Bains JS.** Actions of angiotensin in the subfornical organ and area postrema: implications for long term control of autonomic output. *Clin Exp Pharmacol Physiol* 24: 96–101, 1997.
9. **Gao L, Wang W, Li YL, Schultz HD, Liu D, Cornish KG, Zucker IH.** Superoxide mediates sympathoexcitation in heart failure: roles of angiotensin II and NAD(P)H oxidase. *Circ Res* 95: 937–944, 2004.
10. **Helwig BG, Musch TI, Craig RA, Kenney MJ.** Increased interleukin-6 receptor expression in the paraventricular nucleus of rats with heart failure. *Am J Physiol Regul Integr Comp Physiol* 292: R1165–R1173, 2007.
11. **Heymans S, Luttun A, Nuyens D, Theilmeier G, Creemers E, Moons L, Dyspersin GD, Cleutjens JP, Shipley M, Angellilo A, Levi M, Nube O, Baker A, Keshet E, Lupu F, Herbert JM, Smits JF, Shapiro SD, Baes M, Borgers M, Collen D, Daemen MJ, Carmeliet P.** Inhibition of plasminogen activators or matrix metalloproteinases prevents cardiac rupture but impairs therapeutic angiogenesis and causes cardiac failure. *Nat Med* 5: 1135–1142, 1999.
12. **Huang BS, Ahmad M, Tan J, Leenen FH.** Sympathetic hyperactivity and cardiac dysfunction post-MI: different impact of specific CNS versus general AT1 receptor blockade. *J Mol Cell Cardiol* 43: 479–486, 2007.
13. **Leenen FH.** Brain mechanisms contributing to sympathetic hyperactivity and heart failure. *Circ Res* 101: 221–223, 2007.
14. **Lindley TE, Doobay MF, Sharma RV, Davisson RL.** Superoxide is involved in the central nervous system activation and sympathoexcitation of myocardial infarction-induced heart failure. *Circ Res* 94: 402–409, 2004.

15. **Lu N, Helwig BG, Fels RJ, Parimi S, Kenney MJ.** Central Tempol alters basal sympathetic nerve discharge and attenuates sympathetic excitation to central ANG II. *Am J Physiol Heart Circ Physiol* 287: H2626–H2633, 2004.
16. **Lutgens E, Daemen MJ, de Muinck ED, Debets J, Leenders P, Smits JF.** Chronic myocardial infarction in the mouse: cardiac structural and functional changes. *Cardiovasc Res* 41: 586–593, 1999.
17. **Mani K.** Programmed cell death in cardiac myocytes: strategies to maximize post-ischemic salvage. *Heart Fail Rev* 13: 193–209, 2008.
18. **Martinka P, Fielitz J, Patzak A, Regitz-Zagrosek V, Persson PB, Stauss HM.** Mechanisms of blood pressure variability-induced cardiac hypertrophy and dysfunction in mice with impaired baroreflex. *Am J Physiol Regul Integr Comp Physiol* 288: R767–R776, 2005.
19. **Pocock S, Wilhelmsen L, Dickstein K, Francis G, Wittes J.** The data monitoring experience in the MOXCON trial. *Eur Heart J* 25: 1974–1978, 2004.
20. **Rosamond W, Flegal K, Furie K, Go A, Greenlund K, Haase N, Hailpern SM, Ho M, Howard V, Kissela B, Kittner S, Lloyd-Jones D, McDermott M, Meigs J, Moy C, Nichol G, O'Donnell C, Roger V, Sorlie P, Steinberger J, Thom T, Wilson M, Hong Y, American Heart Association Statistics Committee and Stroke Statistics Subcommittee.** Heart Disease and Stroke Statistics 2008 Update A Report From the American Heart Association Statistics Committee and Stroke Statistics Subcommittee [Online]. *Circulation* 117: e25–e146, 2008.
21. **Sinnayah P, Lindley TE, Staber PD, Davidson BL, Cassell MD, Davisson RL.** Targeted viral delivery of Cre recombinase induces conditional gene deletion in cardiovascular circuits of the mouse brain. *Physiol Genomics* 18: 25–32, 2004.
22. **Spinale FG.** Myocardial matrix remodeling and the matrix metalloproteinases: influence on cardiac form and function. *Physiol Rev* 87: 1285–1342, 2007.
23. **Sun Y.** Oxidative stress and cardiac repair/remodeling following infarction. *Am J Med Sci* 334: 197–205, 2007.
24. **Suzuki Y, Nakano K, Sugiyama M, Imagawa J.** betaARK1 inhibition improves survival in a mouse model of heart failure induced by myocardial infarction. *J Cardiovasc Pharmacol* 44: 329–334, 2004.
25. **Watson AM, Hood SG, May CN.** Mechanisms of sympathetic activation in heart failure. *Clin Exp Pharmacol Physiol* 33: 1269–1274, 2006.
26. **Wencker D, Chandra M, Nguyen K, Miao W, Garantziotis S, Factor SM, Shirani J, Armstrong RC, Kitsis RN.** A mechanistic role for cardiac myocyte apoptosis in heart failure. *J Clin Invest* 111: 1497–1504, 2003.
27. **Westermann D, Mersmann J, Melchior A, Freudenberger T, Petrik C, Schaefer L, Lullmann-Rauch R, Lettau O, Jacoby C, Schrader J, Brand-Herrmann SM, Young MF, Schultheiss HP, Levkau B, Baba HA, Unger T, Zacharowski K, Tschope C, Fischer JW.** Biglycan is required for adaptive remodeling after myocardial infarction. *Circulation* 117: 1269–1276, 2008.
28. **Yu Y, Zhang ZH, Wei SG, Chu Y, Weiss RM, Heistad DD, Felder RB.** Central gene transfer of interleukin-10 reduces hypothalamic inflammation and evidence of heart failure in rats after myocardial infarction. *Circ Res* 101: 304–312, 2007.
29. **Zanzinger J, Czachurski J.** Chronic oxidative stress in the RVLM modulates sympathetic control of circulation in pigs. *Pflügers Arch* 439: 489–494, 2000.
30. **Zhang ZH, Yu Y, Kang YM, Wei SG, Felder RB.** Aldosterone acts centrally to increase brain renin-angiotensin system activity and oxidative stress in normal rats. *Am J Physiol Heart Circ Physiol* 294: H1067–H1074, 2008.
31. **Zhu GQ, Gao L, Li Y, Patel KP, Zucker IH, Wang W.** AT1 receptor mRNA antisense normalizes enhanced cardiac sympathetic afferent reflex in rats with chronic heart failure. *Am J Physiol Heart Circ Physiol* 287: H1828–H1835, 2004.
32. **Zimmerman MC, Lazartigues E, Lang JA, Sinnayah P, Ahmad IM, Spitz DR, Davisson RL.** Superoxide mediates the actions of angiotensin II in the central nervous system. *Circ Res* 91: 1038–1045, 2002.
33. **Zimmerman MC, Lazartigues E, Sharma RV, Davisson RL.** Hypertension caused by angiotensin II infusion involves increased superoxide production in the central nervous system. *Circ Res* 95: 210–216, 2004.
34. **Zimmerman MC, Dunlay RP, Lazartigues E, Zhang Y, Sharma RV, Engelhardt JF, Davisson RL.** Requirement for rac1-dependent NADPH oxidase in the cardiovascular and dipsogenic actions of angiotensin II in the brain. *Circ Res* 95: 532–539, 2004.
35. **Zucker IH.** Novel mechanisms of sympathetic regulation in chronic heart failure. *Hypertension* 48: 1005–1011, 2006.